A computational journey in the CH2O2S land: an accurate rotational and ro-vibrational analysis of the sulfene molecule and the O,S- and O,O-monothiocarbonic acids

# A Computational Journey in the $CH_2O_2S$ Land: An Accurate Rotational and Ro-vibrational Analysis of the Sulfene molecule and the O,S- and O,O-Monothiocarbonic Acids

S. Alessandrini[a,b], V. Dell'Isola[b], L. Spada[a,b], V. Barone[a] and C. Puzzarini[b]

[a]Scuola Normale Superiore, Piazza dei Cavalieri 7, I-56126 Pisa, Italy; [b]Dipartimento di Chimica "Giacomo Ciamician", Università di Bologna, Via F. Selmi 2, I-40126 Bologna, Italy.

**ARTICLE HISTORY**
Compiled May 5, 2020

**ABSTRACT**

Molecules containing sulfur play an important role in atmospheric chemistry, but their reactivity in such environment is far from being well characterised. Therefore, important transient species might still have to be disclosed. In this regard, this paper aims at contributing to this field by means of the computational spectroscopic characterisation of potentially relevant atmospheric species, such as the $CH_2O_2S$ isomers. Based on our computational investigation, the most stable species are the carbonothionic O,S- and O,O-acids. In addition to them, the sulfene molecule has also been considered. For all these species, the equilibrium structure and the corresponding rotational constants have been accurately evaluated using a coupled-cluster-based composite approach. All the other parameters required for the simulation of the rotational and ro-vibrational spectra have been obtained by exploiting density functional theory.

**KEYWORDS**
Spectroscopic Characterisation; ab initio Methods; Atmospheric Chemistry; Sulfur-containing compounds; Computational Spectroscopy

## 1. Introduction

Sulfur-bearing molecules are widespread in our atmosphere in two forms: reduced sulfur gases and their oxidised forms. The ubiquity of reduced sulfur compounds, such as dimethyl sulfide (DMS) or carbon disulfide ($CS_2$), is related to several biogenic reactions, from those occurring in soils and marshland to those taking place in marine waters due to phytoplankton. Instead, the presence of oxidised form of sulfur (e.g. $SO_2$) is mostly due to anthropogenic sources, like the combustion of oil and its derivatives [1, 2]. In particular, the anthropogenic sources are nowadays of the same entity as the natural ones, thus significantly affecting the sulfur budget of the atmosphere. Indeed, once sulfur compounds are delivered in the atmosphere they undergo different reactions, thus establishing the so-called "sulfur-cycle". The reduced species are quickly oxidised to sulfur dioxide and then to ${SO_4}^{2-}$, which is responsible for acid rains and

Corresponding author S. A. Email: silvia.alessandrini@sns.it
Corresponding author C. P. Email: cristina.puzzarini@unibo.it

aerosols. While these processes occur in the troposphere, sulfur is also able to reach the stratosphere thanks to the long lifetime of COS. There, the sulfur-layer influences the local temperature and the ozone concentration [2, 3].

The reaction mechanisms entering the sulfur-cycle have not been fully understood yet and other important transient species and/or intermediates may be present in the atmosphere. In this regard, interesting molecules not investigated yet are those belonging to the $CH_2O_2S$ isomers, such as the monothiocarbonic acids and the sulfene molecule [4]. The former, the mono-sulfur analogue of carbonic acid, was proposed as an intermediate of the gas-phase reaction between $H_2S$ and $CO_2$, with COS being the final product. The energetic barriers involved in this reaction are also easily lowered down thanks to organocatalysis, which could be due to amine or acids of different nature, like the monothiocarbonic acid itself. As a consequence, this reaction can be an interesting process also occurring in Venus's atmosphere [5].

A second interesting $CH_2O_2S$ isomer is sulfene (or thioformaldehyde-S,S-dioxide). Little is known about this molecule, possibly due to its high reactivity it can undergo polymerisation and it is able to easily decompose to formaldehyde and sulfur monoxide [6–8]. However, sulfene and it derivatives ($R_1R_2SO_2$, with $R_1$ and $R_2$ being two generic substituents), play an important role in organic chemistry, thereby being used for Diels-Alder reactions [9, 10]. Furthermore, sulfene is expected to be one of the major products of the reaction between $CH_3SO_2$ and halogen monoxide radicals (XO with X = F, Cl and Br) [11]. This is a key reaction because $CH_3SO_2$ is present in the atmosphere as one of the fundamental intermediates of dimethyl sulfide oxidation and it is able to react with oxidant species such as $O_3$ or $NO_x$ [12]. Therefore, the reaction with halogen monoxide radicals, which are oxidant molecules present in the troposphere, is likely to occur [11].

The identification of a given molecule in the atmosphere is based on spectroscopic analyses that involve radiations ranging from the microwave region to the ultraviolet. In this context, pivotal are high-resolution spectroscopic techniques, such as rotational and ro-vibrational spectroscopies, which allow for the determination of various physical-chemical parameters that, in turn, are used for modelling radiative atmospheric processes. For example, HITRAN [13] is the most known spectroscopic database collecting all the line-by-line parameters and information required to predict and simulate the transmission and emission of light in the atmosphere. While the spectroscopic data needed in the atmospheric spectra simulations are usually derived from experimental measurements [14], it is not always possible to study, for example, the ro-vibrational spectrum of unstable species like radicals. In such cases, computational spectroscopy combined with state-of-the-art quantum-chemical methodologies play an important role in providing accurate predictions of spectroscopic parameters, such as rotational constants and vibrational frequencies [15–17].

In this context, the aim of this paper is the accurate simulation of the rotational and ro-vibrational spectra of isomers/conformers of the monothiocarbonic acid as well as of the sulfene molecule. In the next section, the computational methodology is detailed. Subsequently, the results are discussed with special focus on the spectral features of sulfene and the most stable $CH_2O_2S$ isomers. In the last section, conclusions are outlined with emphasis on the future work.

## 2. Computational Methodology

The present computational investigation has been based on density functional theory and coupled-cluster methodologies. Concerning the former, the double-hybrid B2PLYP functional [18], including the D3 dispersion correction [19] combined with the Becke-Johnson dumping function (B2PLYP-B3BJ) [20], has been employed. Moving to the coupled-cluster (CC) theory [21], the CC method that accounts for single and double excitations (CCSD) and a perturbative treatment of connected triples, namely CCSD(T) [22], has been used. All the DFT computations have been carried out using the Gaussian16 suite of programs [23], while the CFour program package [24] has been employed for CC calculations.

The B2PLYP-D3BJ functional in conjunction with the minimally-augmented triple-$\zeta$ basis set [25] without $d$-functions on hydrogen atoms (maug-cc-pVTZ-$d$H) [26] has been used to investigate the $CH_2O_2S$ potential energy surface (PES), within the Born-Oppenheimer approximation, in order to locate all stable isomers (minima). This implies that geometry optimisations, carried out at the B2PLYP-D3BJ/maug-cc-pVTZ-$d$H level of theory (hereafter shortly denoted as B2-D3), have been followed by harmonic force-field calculations at the same level to check the nature of the stationary point. The latter computations also provide the harmonic zero-point energy (ZPE) corrections.

Based on the preliminary B2-D3 calculations, the relative stability of the several isomers located on the PES together with their conformers has been derived (see Figure S1 and S2 in the Supplementary Information, SI). Among these 33 stable structures, two tautomeric forms of the monothiocarbonic acid, namely the carbonothionic O,S-acid [OC(OH)(SH)] and the carbonothionic O,O-acid [$SC(OH)_2$], as well as the sulfene molecule [$SO_2CH_2$] have been selected for a more accurate characterisation. For the former, all four conformers of the O,S-acid and all three conformers of the O,O-acid have been considered, which all lie well within 100 kJ mol$^{-1}$ (see Figure 1). In a second step, their equilibrium geometries have been accurately determined by means of the so-called "CCSD(T)/CBS+CV" composite scheme [27, 28] (hereafter simply denoted as CBS+CV), which is an energy gradient approach. This means that the CBS+CV equilibrium structure has been obtained by minimising the following energy gradient:

$$\frac{dE_{\mathrm{CBS}}}{dx} = \frac{dE^{CBS}(\mathrm{HF-SCF})}{dx} + \frac{d\Delta E^{CBS}(\mathrm{CCSD(T)})}{dx} + \frac{d\Delta E_{CV}}{dx} \ , \qquad (1)$$

where the first two terms on the right-hand side are the energy gradients obtained using the exponential extrapolation formula introduced by Feller [29] and the two-point $n^{-3}$ expression by Helgaker *et al.* [30] for the Hartree-Fock self consistent field (HF-SCF) energy and the CCSD(T) correlation contribution, respectively. The cc-pV($n+d$)Z basis sets [31–33] have been employed, with $n$=T, Q and 5 being chosen for the HF-SCF extrapolation and $n$=T and Q being used for CCSD(T). Core-valence correlation effects have been considered by adding the corresponding correction, $d\Delta E_{CV}/dx$, where the all-electron and frozen-core energy difference is evaluated employing the cc-pwCVTZ basis set [34]. As a by-product of CBS+CV geometry optimisations, the electronic energies have been evaluated at the same level of theory.

Moving to the spectroscopic characterisation, the equilibrium rotational constants are straightforwardly obtained from the equilibrium structure. However, despite the fact that the equilibrium term provides by far the most important contribution [28, 35], vibrational corrections need to be incorporated to accurately predict rotational

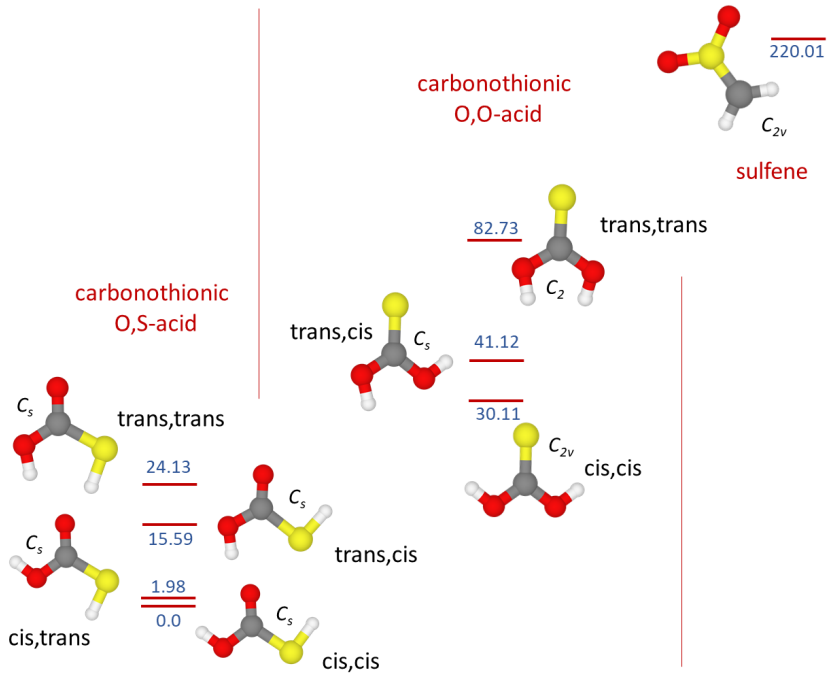


**Figure 1.** CBS+CV+ZPE relative energies (kJ mol$^{-1}$) of the conformers of carbonothionic O,S- and O,O-acids, and sulfene (see Table 1).

constants for a given vibrational states. This is accomplished by exploiting second-order vibrational perturbation theory (VPT2) [36–39], thus leading to the following expression for the rotational constant of a generic v-th vibrational state ($B^i_{\mathrm{v}}$):

$$B^i_{\mathrm{v}} = B^i_e - \sum_r \alpha^i_r \left(v_r + \frac{1}{2}\right) \tag{2}$$

where $i$ denotes the inertial axis ($i = a, b, c$, so that $B^a_{\mathrm{v}} = A_{\mathrm{v}}$) and the sum runs over all normal coordinates ($r$), with $v_r$ being the corresponding vibrational quantum number. In eq. 2, $B^i_e$'s are the equilibrium rotational constants and the $\alpha^i_r$'s are the vibration-rotation constants, which consist of three contributions, the anharmonic one being by far the largest one. Therefore, anharmonic force-field calculations are required [35]. As a by-product of such computations, quartic and sextic centrifugal distortion constants are also obtained. These represent additional crucial parameters for the accurate simulation of rotational spectra [35]. Since the evaluation of a cubic force field is computationally expensive, we resorted to the B2-D3 level, which is proved to provide accurate results in this respect (see, e.g., refs. [40–43]). In passing we note that, according to eq. 2, vibrational corrections do not vanish even for the vibrational ground state. Finally, to simulate rotational spectra, the knowledge of the dipole moment is required. In fact, its components along the inertial axes provide the information on which types of transitions are allowed and on their intensity.

To simulate ro-vibrational spectra, in addition to the rotational parameters of all vibrational states involved in the transitions considered, the anharmonic vibrational frequencies and the corresponding infrared (IR) intensities are required. While – in principle – both frequencies and intensities are obtained from the anharmonic force-

field computations mentioned above, these quantities might be affected by resonances, such as the Fermi ones. For this reason, the generalised formulation of VPT2 (GVPT2) was employed. In the latter, resonant terms are removed and then re-introduced in a subsequent variational treatment [39]. While more details can be found in ref. [39], here we not that these computations also provide the anharmonic ZPE corrections.

As a last remark, it is noted that all the species considered are asymmetric rotors and the $I^r$ representation combined with the $S$ reduction of the Watson Hamiltonian [44, 45] have been chosen for the spectroscopic characterisation. In this work, all spectra simulations have been performed using Pickett's SPCAT program [46], which is embedded in the VMS-ROT software [47].

## 3. Results and Discussion

As mentioned above, among the various stable isomers on the $CH_2O_2S$ PES, all possible conformers of the carbonothionic O,S- and O,O-acids have been investigated in detail, with the former being the most stable tautomer. Despite the fact that various isomers and their conformers lie energetically between the carbonothionic O,O-acid and sulfene (see Figures S1 and S2 in the SI), the latter has been considered because of its potential interest, as outlined in the Introduction. In the following, the relative energy of the most stable $CH_2O_2S$ species is first of all addressed. Then, the spectroscopic characterisation for the three classes of compounds selected is reported and discussed.

### *3.1. The relative stability of the $CH_2O_2S$ species*

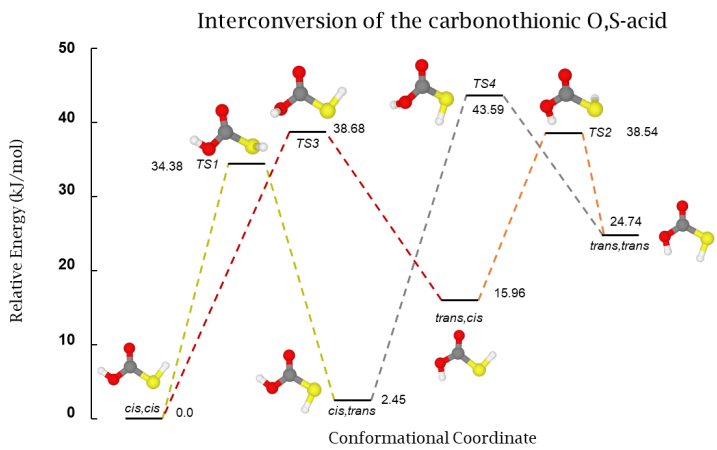


**Figure 2.** B2-D3 relative energies, corrected for the harmonic ZPE at the same level, of the four O,S-acid conformers together with transition states ruling their interconversion.

At the B2-D3 level, the most stable species on the $CH_2O_2S$ PES is the cis,cis conformer of the carbonothionic O,S-acid. Upon out-of-plane rotation of the H–S bond, the cis,trans conformer is obtained, which is the second most stable form and lies about 2 kJ mol$^{-1}$ higher in energy. The out-of-plane rotation of the H–O bond leads instead to the trans,cis conformer, which is even less stable, indeed lying more than 15 kJ mol$^{-1}$ above the global minimum. Finally, the interconversion of both hydrogens leads

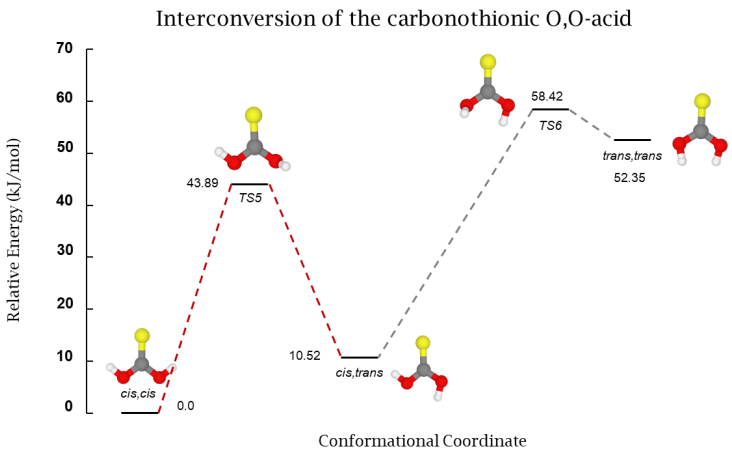


**Figure 3.** B2-D3 relative energies, corrected for the harmonic ZPE at the same level, of the three O,O-acid conformers together with transition states ruling their interconversion.

**Table 1.** Relative energies (kJ mol$^{-1}$) of the carbonothionic O,S- and O,O-acid conformers, and of the sulfene molecule.[a]

| | B2-D3 | CBS | CBS+CV | CBS+CV+ZPE[b] |
|---|---|---|---|---|
| O,S-acid | | | | |
| cis,cis | 0.0 | 0.0 | 0.0 | 0.0 |
| cis,trans | 2.79 | 2.38 | 2.38 | 1.98 |
| trans,cis | 17.15 | 16.61 | 16.63 | 15.59 |
| trans,trans | 26.71 | 25.67 | 25.74 | 24.14 |
| O,O-acid | | | | |
| cis,cis | 23.39 | 20.92 | 21.01 | 30.11 |
| cis,trans | 35.27 | 33.17 | 33.28 | 41.12 |
| trans,trans | 80.28 | 78.09 | 78.39 | 82.73 |
| sulfene | 225.50 | 219.71 | 218.60 | 220.01 |

[a] Reference structures: CBS+CV for CBS and CBS+CV energies, B2-D3 for B2-D3 energies. [b] ZPE anharmonic corrections at the B2-D3 level.

to the trans,trans conformer, whose relative energy is ∼24 kJ mol$^{-1}$. In Figure 2, the four conformers of the carbonothionic O,S-acid are shown together with the transition states ruling their interconversion, while the relative energies of the minima computed at different levels of theory are collected in Table 1. The isomerisation from the carbonothionic O,S-acid to the O,O tautomer requires an hydrogen migration from sulfur to oxygen and this process has an energy barrier of ∼142 kJ mol$^{-1}$ according to ref. [4]. Also for the O,O isomer, the cis,cis form is the most stable conformer, which – however – lies ∼30 kJ mol$^{-1}$ above the O,S-analogous. Analogously to the carbonothionic O,S-acid, the conformational modifications occur upon out-of-plane rotations of H–O bonds. Once again, the trans,cis form is more stable than the trans,trans conformer by about 41 kJ mol$^{-1}$, with the trans,cis form lying ∼11 kJ mol$^{-1}$ above the cis,cis conformer. These three conformers are shown in Figure 3 together with the transition states ruling their interconversion, while the energies of the minima at different levels of theory are given in Table 1. The sulfene molecule exists instead in only one form, which is unrelated to the monothiocarbonic acids. The B2-D3 structures of all the species discussed above are reported in the SI.

The CCSD(T)/CBS electronic energies (see Table 1) agree well with the results at the B2-D3 level, the discrepancies being well within 1-2 kJ mol$^{-1}$, with sulfene being the only exception (in this case the difference is $\sim$6 kJ mol$^{-1}$). This further confirms the reliability and accuracy of the B2-D3 level of theory. The inclusion of the core-correlation correction (thus leading to the CBS+CV level) determines a small increase of the relative energy for all species but sulfene, with the largest contribution amounting to 0.3 kJ mol$^{-1}$. Indeed, for the latter species, the CV correction decreases the relative energy by about 1.1 kJ mol$^{-1}$. Adding the B2-D3 anharmonic ZPE corrections leaves the general trend unchanged, with contributions ranging from less than 1 kJ mol$^{-1}$ to more than 9 kJ mol$^{-1}$. While within the O,S-acid family inclusion of ZPE decreases the relative energies, the opposite occurs for the O,O-acid conformers. A note on the anharmonic ZPE corrections is appropriate here. In fact, it has to be noted that a resonance-free expression [48] was used for their computation.

The estimates of Table 1 represent the most accurate energetic data currently reported in the literature for the species under investigation. Indeed, while in reasonable good agreement, our results provide a relevant improvement with respect to the values reported in ref. [4], which were obtained at the CCSD(T)/cc-pVQZ level of theory on top of CCSD(T)/cc-pVTZ optimised geometries.

### *3.2. Rotational and ro-vibrational spectroscopy*

While the specific results for the various species considered will be detailed in the next sections, here we discuss the accuracy of the computed spectroscopic parameters and of the rotational and ro-vibrational spectra issuing from them.

According to ref. [28], the equilibrium rotational constants obtained at the CBS+CV level of theory have a mean deviation from the experimental values of 0.5%, which is further reduced to 0.3% if the vibrational corrections are incorporated. This means that the rotational constants obtained in this study should be sufficiently accurate for simulating the corresponding rotational spectra, and especially the low frequency transitions [49]. However, to have reliable simulations also for high-$J$ values, the centrifugal distortion constants have to be considered. Usually, the computed quartic and sextic centrifugal distortion constants have an accuracy of a few-percents (1-10%) and are suitable for simulating spectra that aim at guiding experimental measurements [35]. The last quantity needed to simulate rotational spectra is the dipole moment, which strongly influences the transition intensities. However, the experimental intensity is affected by several factors and the computed values are indeed employed to determine the frequency regimes where the most intense transitions lie. In this study, the vibrationally corrected dipole moment components are used and these have been taken from B2-D3 anharmonic calculations and are all reported in the SI.

To simulate the ro-vibrational spectra, in addition to the previous parameters, the vibrational frequencies and the relative intensities are also required. Both quantities have been obtained at the B2-D3 level and an accuracy of 10 to 20 cm$^{-1}$ is expected for the vibrational energies [26]. In the following, only the most intense bands have been reported in the spectra simulations, with the arbitrary choice of reporting only the three or four fundamental bands with highest intensity, according to our computations. To obtain the rotational constants of the v-th vibrational state, the equilibrium rotational constants have been corrected according to equation 2. However, due to the lack of the corresponding implementation, the centrifugal distortion constants of all vibrational levels have been kept fixed at the equilibrium values, i.e. those employed for

the rotational spectra simulations. The rotational constants of the excited vibrational states are reported in the SI.

### *3.2.1. Sulfene*

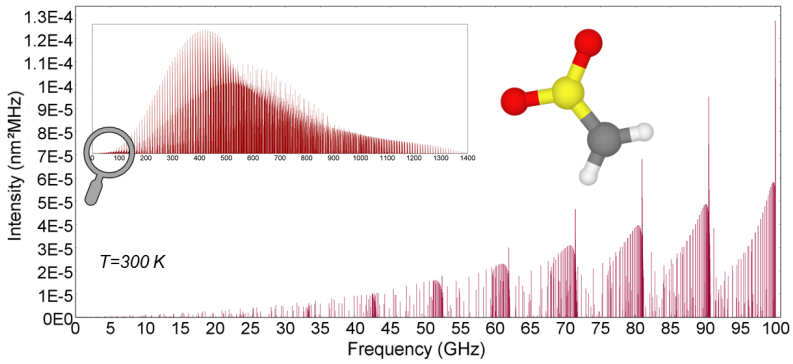


**Figure 4.** Rotational spectrum of sulfene in the 0-100 GHz range at T=300 K. In the inset, the full spectrum (0-1.4 THz) at the same temperature is depicted.

The equilibrium structural parameters of sulfene, obtained at the CBS+CV level, are collected in Table 2. These provide the most accurate estimate of the sulfene geometry currently reported in literature. The C=S distance is 1.5806 Å and, thus, it is similar to that of the isothiocyanic acid [50]. The bond between sulfur and oxygen is in agreement with the typical distance in the $SO_2$ molecule, which has a bond distance of 1.4302 Å at the "fc-CCSD(T)/CBS(Q,5)+ core(cc-pCVTZ)" level (from ref. [28]). However, the ∠OSO angle is slightly larger than that of $SO_2$ (121.86° vs 119.24°). The HCS angle amounts to 117.4°, thus confirming that the carbon is effectively involved in a double bond with the sulfur atom.

The computed rotational spectrum of sulfene (point group $C_{2v}$) is reported in Figure 4 and was simulated using the spectroscopic parameters reported in Table 2, at a temperature of 300 K. Sulfene is a near-oblate rotor and, due to its symmetry, its dipole moment lies along the $a$ axis. Therefore, its rotational spectrum consists of $a$-type transitions. In the inset of Figure 4, the entire spectrum of $CH_2SO_2$ is depicted. It is noted that the maximum intensity is reached at ∼400 GHz. However, the computed transitions are more reliable at lower frequencies. For this reason, the range between 0 and 100 GHz is shown in more details. According to ref. [28], in this range, the discrepancies between computed and experimental transition frequencies can be as low as 0.03% in terms of relative error, which is an accuracy well suited to guide experimental measurements.

The ro-vibrational spectrum of $CH_2SO_2$ in depicted in Figure 5, where the three most intense vibrational bands, i.e. $\nu_3$, $\nu_7$ and $\nu_{10}$, are reported. The $\nu_7$ vibration has $B_1$ symmetry and it corresponds to the wagging of the two hydrogens bonded to the carbon atom. Therefore, it breaks the planar symmetry of the molecule giving rise to a $c$-type band contour. The harmonic frequency is 656.20 cm$^{-1}$, which lowers to 642.98 cm$^{-1}$ when anharmonicity is introduced, while the intensity remains nearly unchanged (from 70 to 65 km mol$^{-1}$). This vibrational mode is shown in detail in the inset of Figure 5, with the P, Q and R branches being well evident.

Going to higher energies, the two most intense vibrational bands are predicted to lie at 1228.51 cm$^{-1}$ ($\nu_3$) and 1368.13 cm$^{-1}$ ($\nu_{10}$). The former fundamental, of $A_1$ sym-

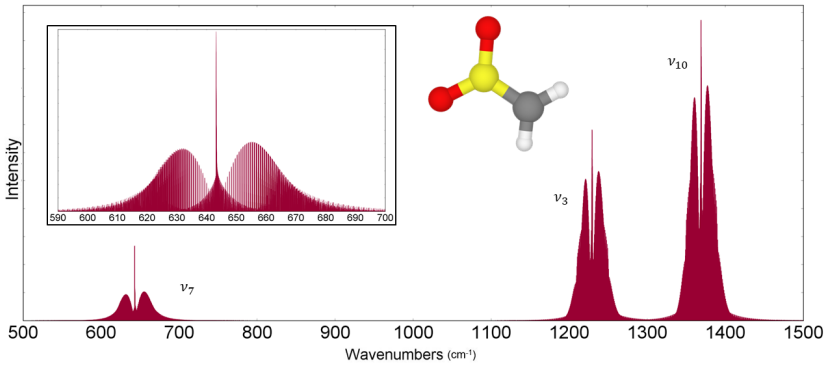


**Figure 5.** Ro-vibrational spectrum of sulfene: its three most intense vibrational bands ($\nu_3$, $\nu_7$ and $\nu_{10}$) are shown. Intensity is in arbitrary unit.

**Table 2.** Structural[a] and spectroscopic[b] parameters of sulfene.

| Parameter[c] | Theoretical value | Parameter[c] | Theoretical value | Parameter[c] | Harm. value | Anharm. value |
|---|---|---|---|---|---|---|
| $r_{\mathrm{SO}}$ | 1.4258 | $D_J$ | $8.53 \times 10^{-3}$ | $\nu_1$ | 3209.53 (14.9) | 3086.63 (12.2) |
| $r_{\mathrm{SC}}$ | 1.5806 | $D_{JK}$ | $-1.51\times 10^{-2}$ | $\nu_2$ | 1397.46 (41.0) | 1397.39 (8.7) |
| $r_{\mathrm{CH}}$ | 1.0748 | $D_K$ | $7.05 \times 10^{-3}$ | $\nu_3$ | 1252.66 (54.8) | 1228.51 (125.0) |
| $\angle$OCS | 119.07 | $d_1$ | $-1.59 \times 10^{-4}$ | $\nu_4$ | 962.54 (3.7) | 941.13 (2.2) |
| $\angle$HCS | 117.40 | $d_2$ | $-3.96 \times 10^{-4}$ | $\nu_5$ | 495.78 (30.9) | 492.03 (30.1) |
| $A_{\mathrm{e}}$ | 9810.72 | $H_J$ | $1.91 \times 10^{-8}$ | $\nu_6$ | 608.70 (0.0) | 593.03 (0.0) |
| $B_{\mathrm{e}}$ | 9358.31 | $H_K$ | $-3.92 \times 10^{-8}$ | $\nu_7$ | 656.20 (70.1) | 642.98 (65.4) |
| $C_{\mathrm{e}}$ | 4789.59 | $H_{JK}$ | $-7.74 \times 10^{-8}$ | $\nu_8$ | 379.29 (31.1) | 372.23 (30.1) |
| $\Delta A_{\mathrm{vib}}$ | -30.07 | $H_{KJ}$ | $9.75 \times 10^{-8}$ | $\nu_9$ | 3347.99 (16.3) | 3205.12 (12.5) |
| $\Delta B_{\mathrm{vib}}$ | -59.41 | $h_1$ | $9.14 \times 10^{-10}$ | $\nu_{10}$ | 1391.32 (92.3) | 1368.13 (176.7) |
| $\Delta C_{\mathrm{vib}}$ | -28.97 | $h_2$ | $-2.34 \times 10^{-9}$ | $\nu_{11}$ | 936.49 (0.7) | 918.10 (0.8) |
| $A_0$ | 9780.65 | $h_3$ | $-6.08 \times 10^{-10}$ | $\nu_{12}$ | 393.33 (3.4) | 391.67 (3.1) |
| $B_0$ | 9298.90 | | | | | |
| $C_0$ | 4760.62 | | | | | |

[a] Distances in Å, angles in degrees. [b] Rotational parameters in MHz, vibrational frequencies in $\mathrm{cm}^{-1}$, and intensities in km $\mathrm{mol}^{-1}$. [c] Geometrical parameters and equilibrium rotational constants at the CBS+CV level. Anharmonic corrections, quartic and sextic centrifugal distortion constants as well as vibrational frequencies and intensities at the B2-D3 level. The intensities are reported in parentheses after the corresponding vibrational frequencies.

metry, corresponds to the stretching of the C=S bond accompanied by simultaneous adjustments of the S=O bonds. Instead, the latter is the asymmetric stretching of the sulfur-oxygen bonds, belonging to the $B_2$ representation. Both vibrations occur in the plane and give rise to hybrid $a/b$ ro-vibrational bands, as shown in Figure 5.

The fundamentals lying at the highest energies reported in Table 2 correspond to the symmetric- and asymmetric- stretching of the two hydrogen atoms ($\nu_1$ and $\nu_9$, respectively), while the lowest frequency band corresponds to a large amplitude motion, with all the atoms involved in an out-of-plane displacement, thus breaking the planar symmetry. In the end, it is important to point out the fact that the $\nu_6$ fundamental, predicted at 593.03 $\mathrm{cm}^{-1}$, is an IR-inactive transition.

### *3.2.2. The carbonothionic O,S-acid conformers*

The accurate equilibrium structures for all the conformers of this family are reported in Table S21 of the SI. The C=O double bond slightly decreases when going from the cis,cis conformer to the trans,trans form, i.e. from 1.1970 Å to 1.1897 Å, while the C–O single bond shows the opposite trend. This indicates that the resonance structure is partially broken and, indeed, the trans,trans conformer is the less stable. The C–S

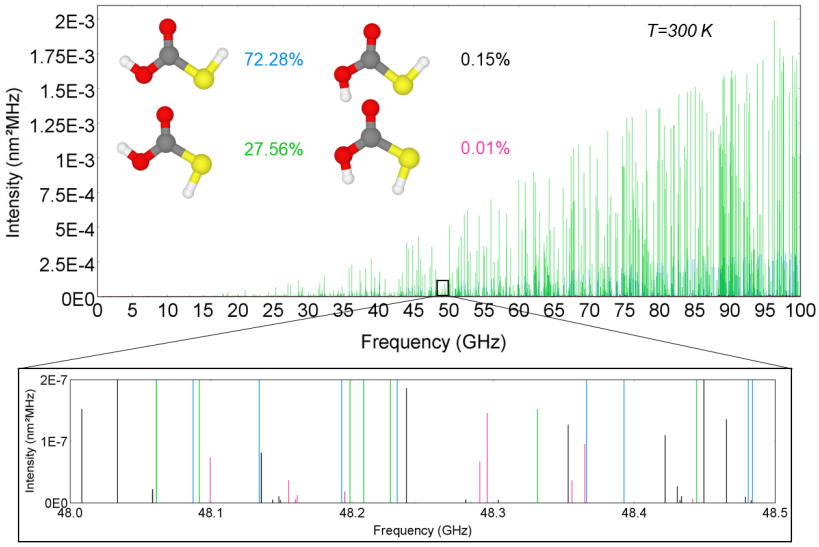


**Figure 6.** Rotational spectra of the four carbonothionic O,S-acid conformers weighted for their Boltzmann population at T=300 K. Top panel: rotational spectrum in the range 0-100 GHz, with the population values being also given. Bottom panel: a zoom of the rotational spectrum in the 48-48.5 GHz range at low intensity.

bond length is 1.7658 Å for the cis,cis conformer, which becomes ∼4 mÅ shorter in the cis,trans conformer. However, this distance increases by about 20 mÅ in the trans,cis and trans,trans conformers, in agreement with their lower stability. The angles are very similar in all conformers, with the largest changes being of 4-5 degrees. Additionally, it should be pointed out that the stability order of the conformers might be correlated to the number and type of intramolecular hydrogen-bonds that are geometrically allowed. This is indeed mirrored in the H–O distances of the various species.

As already mentioned, to this family belong the most stable $CH_2O_2S$ species, with the two low-lying conformers being very close in energy (∼2 kJ mol$^{-1}$). Considering that all the conformers lie within 25 kJ mol$^{-1}$, the rotational spectrum of each species was simulated using the corresponding equilibrium Boltzmann population at T = 300 K and the four rotational spectra were later merged together in Figure 6. The data used for the spectra simulations are reported in Table 3 for the cis,cis conformer, while for the other species they can be found in the SI. The spectrum in Figure 6 shows that, even if the cis,cis conformer is the most stable and its population amounts to ∼73%, the most intense rotational transitions are those belonging to the cis,trans conformer. The reason is that the latter species has a dipole moment one order of magnitude larger than that of the cis,cis form. The other two species, i.e. the trans,cis and trans,trans conformers, have a negligible population (0.15% and 0.01%, respectively). Therefore, the intensity of their rotational transitions is fairly modest. This is evident in the magnification of Figure 6, which shows a small portion of spectrum (0.5 GHz) at low intensity. The pink transitions correspond to the trans,trans conformer and the black ones to the trans,cis species, while the out of scale transitions –blue and green lines– belong to the cis,cis and cis,trans conformers, respectively. Roughly, it can be said that the intensity of the rotational transitions of the less abundant conformers at T = 300 K is four orders of magnitude lower than that of the most stable species.

The ro-vibrational spectrum of the cis,cis conformer is reported in Figure 7, where the $\nu_1$, $\nu_3$, $\nu_5$, and $\nu_{11}$ bands, which are the most intense fundamentals according

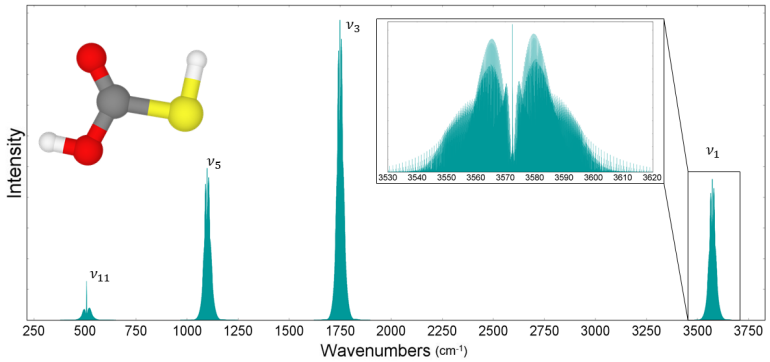


**Figure 7.** Ro-vibrational spectrum of the cis,cis-carbonothionic O,S-acid: the four most intense fundamental bands are depicted. Intensity is in arbitrary unit.

**Table 3.** Rotational[a] and vibrational[b] spectroscopic parameters of the cis,cis carbonothionic O,S-acid.

| Parameter[c] | Theoretical value | Parameter[c] | Theoretical value | Parameter[c] | Harm. value | Anharm. value |
|---|---|---|---|---|---|---|
| $A_e$ | 11668.39 | $D_J$ | $1.12 \times 10^{-3}$ | $\nu_1$ | 3755.98 (101.3) | 3571.36 (86.3) |
| $B_e$ | 5186.03 | $D_{JK}$ | $7.93 \times 10^{-3}$ | $\nu_2$ | 2733.93 (2.8) | 2621.46 (2.1) |
| $C_e$ | 3590.31 | $D_K$ | $2.53 \times 10^{-3}$ | $\nu_3$ | 1781.64 (407.1) | 1747.50 (378.3) |
| $\Delta A_{vib}$ | -80.82 | $d_1$ | $-4.72 \times 10^{-4}$ | $\nu_4$ | 1331.36 (53.2) | 1298.46 (37.5) |
| $\Delta B_{vib}$ | -26.01 | $d_2$ | $-1.63 \times 10^{-4}$ | $\nu_5$ | 1133.11 (334.9) | 1097.51 (304.6) |
| $\Delta C_{vib}$ | -23.65 | $H_J$ | $-2.50\times 10^{-10}$ | $\nu_6$ | 937.41 (74.6) | 921.55 (67.5) |
| $A_0$ | 11587.57 | $H_K$ | $-4.36\times 10^{-8}$ | $\nu_7$ | 724.38 (87.3) | 713.86 (63.7) |
| $B_0$ | 5160.02 | $H_{JK}$ | $-3.90\times 10^{-10}$ | $\nu_8$ | 483.13 (7.4) | 476.99 (5.9) |
| $C_0$ | 3566.66 | $H_{KJ}$ | $6.12\times 10^{-8}$ | $\nu_9$ | 359.54 (3.1) | 357.01 (3.3) |
| | | $h_1$ | $1.20\times 10^{-10}$ | $\nu_{10}$ | 693.68 (40.9) | 677.14 (21.1) |
| | | $h_2$ | $3.71\times 10^{-10}$ | $\nu_{11}$ | 529.88 (99.3) | 507.69 (103.6) |
| | | $h_3$ | $1.72\times 10^{-10}$ | $\nu_{12}$ | 336.39 (2.5) | 349.60 (2.2) |

[a] Rotational parameters in MHz [b] Vibrational frequencies in $cm^{-1}$, intensities in km $mol^{-1}$ [c] Equilibrium rotational constants at the CBS+CV level. Anharmonic corrections, quartic and sextic centrifugal distortion constants as well as vibrational frequencies and intensities at the B2-D3 level. The intensities are reported in parentheses after the corresponding vibrational frequencies.

to our computations (Table 3), are depicted. The most intense transition (378.3 km $mol^{-1}$) is the one associated to the C=O stretching ($\nu_3$) predicted at 1747.50 $cm^{-1}$, thus lying in the typical C=O stretching region of carboxylic acids. This band has an $A'$ symmetry and it gives rise to both $a$- and $b$-type transitions. To the same symmetry belong also the $\nu_5$ (1097.509 $cm^{-1}$) and $\nu_1$ (3571.36 $cm^{-1}$) bands, which are due to the O–C stretching and O–H stretching, respectively. The former has an intensity of 334.9 km $mol^{-1}$ within the harmonic approximation, which lowers down to 304.6 km $mol^{-1}$ at the anharmonic level. The $\nu_1$ band is predicted to be less intense, with an anharmonic value of 86.3 km $mol^{-1}$. The last band shown in this figure is the $\nu_{11}$ fundamental, which has an $A''$ symmetry and corresponds to the out-of-plane displacement of the H(O) atom. Therefore, this vibrational mode gives rise to a $c$-type contour. As a final notice, from the vibrational frequencies collected in Table 3, it is seen that the $\nu_{12}$ fundamental has a small positive correction (10 $cm^{-1}$) going from the harmonic to the anharmonic value. However, this is an acceptable correction within the GVPT2 treatment, also considering the low frequency of this mode ($\sim$350 $cm^{-1}$ at the anharmonic level).

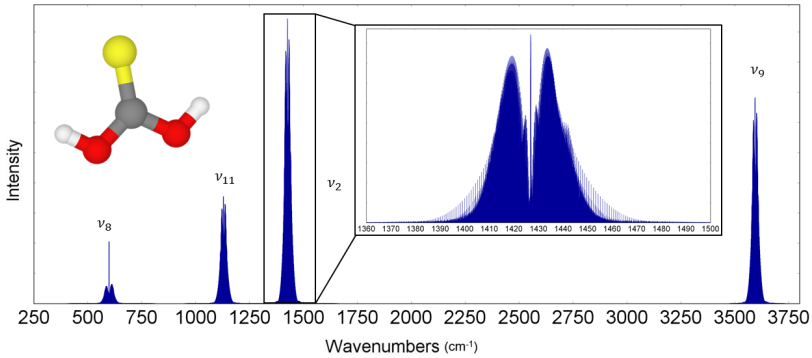


**Figure 8.** Ro-vibrational spectrum of the cis,cis-carbonothionic O,O-acid reporting the most intense bands. Intensity is in arbitrary unit.

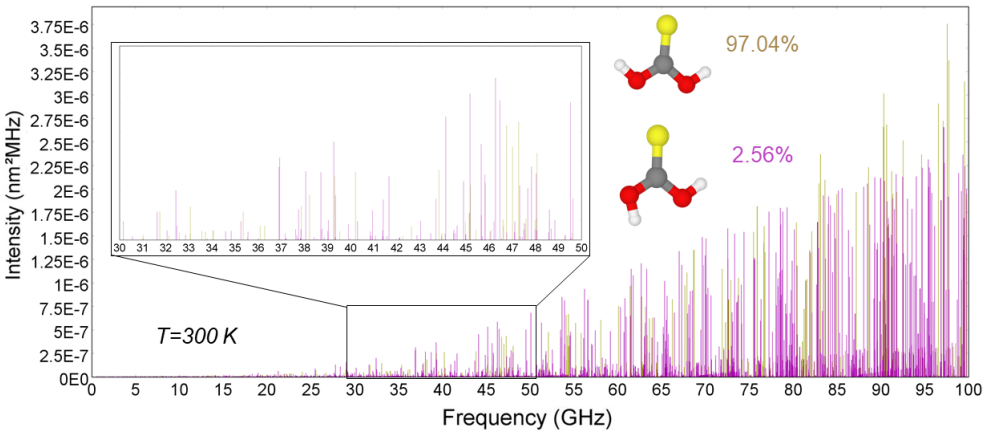


**Figure 9.** Rotational spectra of the cis,cis- and cis,trans-carbonothionic O,O-acids weighted for their Boltzmann population in the 0-10 GHz range at T=300 K. In the inset, the portion between 30 and 50 GHz is shown in detail.

### *3.2.3. The carbonothionic O,O-acid conformers*

The structural parameters for the three conformers of this family are reported in the SI (Table S22). As already noted for the O,S-family, the bond lengths reflect the stability of the cis,cis conformer, with a C=S distance of 1.6367 Å that decreases by ∼1 mÅ in the cis,trans conformer and by 2 mÅ in the trans,trans form. The cis,cis conformer is characterised by a C–O bond length of 1.3226 Å, while for the trans,trans conformer the same distance is 1.3443 Å. However, the cis,trans conformer is characterised by two different C–O distances, with the C–$O_{cis}$ bond length being shorter by 10 mÅ with respect to C–$O_{trans}$. The angles are very similar for all the conformers, with the maximum change occurring for the HOC angle: from 106.72° in the cis,cis conformer to 111.20° for the trans,trans species.

The ro-vibrational spectrum of the cis,cis-carbonothionic O,O-acid is displayed in Figure 8, where the inset shows the P, Q, and R branches of the $\nu_2$ band. According to Table 4, the latter is the most intense band and it corresponds to the in-plane scissoring of the hydrogen atoms. Its harmonic frequency is predicted to be 1464.41 $cm^{-1}$, which is lowered by 38 $cm^{-1}$ at the anharmonic level. This vibrational mode occurs in the molecular plane, thus giving rise to a hybrid $a/b$-type band. The lowest

**Table 4.** Rotational[a] and vibrational[b] spectroscopic parameters of the cis,cis-carbonothionic O,O-acid.

| Parameter[c] | Theoretical value | Parameter[c] | Theoretical value | Parameter[c] | Harm. value | Anharm. value |
|---|---|---|---|---|---|---|
| $A_e$ | 11562.13 | $D_J$ | $8.18 \times 10^{-4}$ | $\nu_1$ | 3790.64 (0.7) | 3597.17 (0.51) |
| $B_e$ | 5307.82 | $D_{JK}$ | $7.82 \times 10^{-3}$ | $\nu_2$ | 1464.41 (652.4) | 1426.33 (613.5) |
| $C_e$ | 3621.69 | $D_K$ | $2.92 \times 10^{-3}$ | $\nu_3$ | 1156.69 (69.8) | 1130.23 (43.2) |
| $\Delta A_{vib}$ | -84.78 | $d_1$ | $-3.73 \times 10^{-4}$ | $\nu_4$ | 809.41 (0.4) | 797.03 (0.9) |
| $\Delta B_{vib}$ | -24.07 | $d_2$ | $-1.54 \times 10^{-4}$ | $\nu_5$ | 507.87 (3.5) | 501.67 (3.8) |
| $\Delta C_{vib}$ | -23.76 | $H_J$ | $4.13 \times 10^{-11}$ | $\nu_6$ | 557.21 (0.0) | 531.97 (0.0) |
| $A_0$ | 11477.34 | $H_K$ | $-3.85 \times 10^{-8}$ | $\nu_7$ | 663.43 (3.0) | 655.44 (0.5) |
| $B_0$ | 5282.95 | $H_{JK}$ | $-2.56 \times 10^{-9}$ | $\nu_8$ | 634.25 (191.4) | 598.72 (192.3) |
| $C_0$ | 3613.68 | $H_{KJ}$ | $5.73 \times 10^{-8}$ | $\nu_9$ | 3785.66 (201.1) | 3592.95 (175.8) |
| | | $h_1$ | $1.48 \times 10^{-10}$ | $\nu_{10}$ | 1436.79 (34.8) | 1395.26 (27.9) |
| | | $h_2$ | $2.74 \times 10^{-10}$ | $\nu_{11}$ | 1175.72 (456.9) | 1129.39 (292.2) |
| | | $h_3$ | $1.49 \times 10^{-10}$ | $\nu_{12}$ | 415.19 (22.8) | 411.51 (21.9) |

[a] Rotational parameters in MHz. [b] Vibrational frequencies in $cm^{-1}$, intensities in km $mol^{-1}$. [c] Equilibrium rotational constants at the CBS+CV level. Anharmonic corrections, quartic and sextic centrifugal distortion constants as well as vibrational frequencies and intensities at the B2-D3 level. The intensities are reported in parentheses after the corresponding vibrational frequencies.

in energy band in Figure 8 corresponds to the $\nu_8$ fundamental, which is the wagging of hydrogens. This band has a $B_1$ symmetry and gives rise to *c*-type transitions. However, its intensity is relatively small compared to $\nu_2$, i.e. 200 km $mol^{-1}$ for the former and 613.5 km $mol^{-1}$ for the latter. The $\nu_{11}$ band is predicted to lie at 1129.39 $cm^{-1}$ with an intensity of 292 km $mol^{-1}$. Also in this case, the vibrational mode involves the hydrogen atoms and occurs in the molecular plane (rocking mode). In Figure 8, at $\sim$3600 $cm^{-1}$ lies the $\nu_9$ fundamental, which is the asymmetric stretching of the O–H bonds. The corresponding symmetric mode is close in energy (3597.17 $cm^{-1}$ the latter, 3592.95 $cm^{-1}$ the former), but its intensity is remarkably lower because the symmetric stretching does not produce a significant change of the dipole moment. As a final note, it is important to point out that, as seen for sulfene, the $\nu_6$ fundamental band is IR inactive. The summary of the frequencies and intensities of all fundamental modes is reported in Table 4.

As done for the O,S family, the rotational spectra of the carbonothionic O,O-acid conformers were simulated considering the equilibrium Boltzmann population (Figure 9). Considering the large difference in energy of the species involved, the cis,cis conformer is by far the most abundant at T = 300 K (97%), while the population of cis,trans is only 2.6%. The remaining 0.4% is due to the trans,trans form, which has not been reported in Figure 9 because its transitions have negligible intensity. However, even if the cis,trans conformer is the less abundant, its rotational transitions, in violet, are as intense as those belonging to the cis,cis species (yellow). This is due, similarly to the O,S family, to the fact that the dipole moment of the former is one order of magnitude larger than that of the most stable conformer (cis,cis). The result is a dense rotational spectrum, as shown by the inset of Figure 9, where a small portion of 20 GHz is considered. The rotational parameters used for the simulations are reported in Table 4 for the cis,cis form, while those of the cis,trans and trans,trans conformers are collected in the SI.

## 4. Conclusions

In the present work, the energetic characterisation of several isomers (and associated conformers) of the $CH_2O_2S$ family was carried out using the B2PLYP-D3 functional in conjunction with a basis set of triple-$\zeta$ quality. From this energetic investigation, the most stable species, i.e. the four conformers of the carbonothionic O,S-acid and

the three forms of the carbonothionic O,O-acid, were chosen for a more detailed computational study, which aimed at the accurate determination of their rotational and vibrational spectroscopic parameters. Moreover, in view of its relevance in atmospheric and organic chemistry, the sulfene molecule was also considered. The equilibrium structures for these species were determined at the CBS+CV level of theory, which provides molecular parameters with an accuracy of 0.001–0.002 Å for bond lengths and 0.05–0.1° for angles [51]. The corresponding equilibrium rotational constants are expected to have a relative accuracy of 0.5%, which improves to 0.3% upon consideration of vibrational corrections. The latter together with the vibrational anharmonic frequencies as well as the quartic and the sextic centrifugal distortion constants were obtained at the B2PLYP-D3 level.

The computed spectroscopic parameters were combined together to simulate the rotational spectra of all the species mentioned above, in all cases the intensities of the transitions being weighted for their equilibrium Boltzmann populations at 300 K. For the O,S-family, the simulated spectra have shown that the most intense transitions belong to the cis,trans-carbonothionic-O,S-acid, which is the second most stable conformer, but it has the largest dipole moment. Instead, for the O,O-family, the cis,cis and cis,trans rotational spectra show nearly the same intensity, the former being the most abundant species (97%) but having a smaller dipole moment.

For the most stable conformers of the O,S- and O,O-families and for sulfene, the ro-vibrational spectra were simulated for the most intense fundamental bands. Among these, for the cis,cis-carbonothionic O,S-acid, the most intense fundamental is the C=O stretching at 1747.5 $cm^{-1}$, while that for the cis,cis-carbonothionic O,O-acid corresponds to the scissoring of hydrogen atoms at 1481 $cm^{-1}$. For sulfene, the band with the highest intensity is due to the asymmetric stretching of S=O bonds, lying at 1368.13 $cm^{-1}$.

The spectroscopic parameters obtained in this study will be helpful to guide future experimental measurements to be carried out in the millimetre/sub-millimetre frequency region and/or in the infrared range. Finally, it is worthwhile mentioning that the energetic estimates and structural parameters determined in this work are the most accurate values presently available for the considered species. Furthermore, the present study is the first one reporting a complete analysis of the $CH_2O_2S$ PES.

## 5. Acknowledgement

This study was supported by Bologna University (RFO funds) and by MIUR (Project PRIN 2015, Grant Number 2015F59J3R). The authors thank Dr. Mattia Melosso for the useful discussions.

## References

[1] L.S.S. Nunes, T.M. Tavares, J. Dippel and W. Jaeschke, J. Atmos. Chem. **50**, 79–100 (2005).

[2] T.S. Bates, B.K. Lamb, A. Guenther, J. Dignon and R.E. Stoiber, J. Atmos. Chem. **14**, 315–337 (1992).

[3] R.P. Wayne, *Chemistry of atmospheres. An introduction to the chemistry of the atmospheres of earth, the planets, and their satellites.*, 3rd ed. Oxford/New York, Clarendon Press–Oxford University Press, (1985).

[4] D. Niedek, J.P. Wagner and P.R. Schreiner, J. Anal. Appl. Pyrolysis **124**, 439–445 (2017).

[5] M. Kumar and J.S. Francisco, Chem. Eur. J **22**, 4359–4363 (2016).
[6] S. Lyashchuk, Russ. J. Org. Chem. **37**, 202–206 (2001).
[7] G. Opitz, Angew. Chem. Int. Ed. Engl. **6**, 107–123 (1967).
[8] J.P. Snyder, J. Org. Chem. **38**, 3965–3967 (1973).
[9] M. Manoharan and P. Venuvanalingam, Int. J. Quantum Chem. **66**, 309–322 (1998).
[10] M. Manoharan and P. Venuvanalingam, J. Phys. Org. Chem. **10** (10), 768–776 (1997).
[11] X. Li, L. Meng, Z. Sun and S. Zheng, J. of Mol. Struct.: THEOCHEM **870**, 53 – 60 (2008).
[12] Z. Salta and A.M. Kosmas, Int. J. Quantum Chem. **114**, 1430–1437 (2014).
[13] I.E. Gordon, L.S. Rothman, C. Hill, R.V. Kochanov, Y. Tan, P.F. Bernath, M. Birk, V. Boudon, A. Campargue, K. Chance *et al.*, J. Quant. Spectrosc. Radiat. Transf. **203**, 3–69 (2017).
[14] L. Bizzocchi, F. Tamassia, J. Laas, B.M. Giuliano, C. Degli Esposti, L. Dore, M. Melosso, E. Canè, A.P. Charmet, H.S.P. Müller, H. Spahn, A. Belloche, P. Caselli, K.M. Menten and R.T. Garrod, Astrophys. J. Suppl. S. **233**, 11 (2017).
[15] A. Melli, M. Melosso, N. Tasinato, G. Bosi, L. Spada, J. Bloino, M. Mendolicchio, L. Dore, V. Barone and C. Puzzarini, Astrophys. J. **855**, 123 (2018).
[16] M. Melosso, L. Dore, J. Gauss and C. Puzzarini, submitted to J. Mol. Spectrosc. (submitted).
[17] C. Puzzarini, J. Bloino, N. Tasinato and V. Barone, Chem. Rev. **119**, 8131–8191 (2019).
[18] S. Grimme, J. Phys. Chem. **124**, 034108 (2006).
[19] S. Grimme, J. Antony, S. Ehrlich and H. Krieg, J. Chem. Phys. **132**, 154104 (2010).
[20] S. Grimme, S. Ehrlich and L. Goerigk, J. Comput. Chem. **32**, 1456–1465 (2011).
[21] I. Shavitt and R.J. Bartlett, *Many-Body Methods in Chemistry and Physics*, 1st ed. Cambrige, Cambridge University Press (2009).
[22] K. Raghavachari, G.W. Trucks, J.A. Pople and M. Head-Gordon, Chem. Phys. Lett. **157**, 479–483 (1989).
[23] M.J. Frisch, G.W. Trucks, H.B. Schlegel, G.E. Scuseria, M.A. Robb, J.R. Cheeseman, G. Scalmani, V. Barone, G.A. Petersson, H. Nakatsuji and et al., Gaussian 16 Revision A.03 2016, Gaussian Inc. Wallingford CT.
[24] J.F. Stanton, J. Gauss, L. Cheng, M.E. Harding, D.A. Matthews and P.G. Szalay, CFOUR, Coupled-Cluster techniques for Computational Chemistry, a quantum-chemical program package With contributions from A.A. Auer, R.J. Bartlett, U. Benedikt, C. Berger, D.E. Bernholdt, Y.J. Bomble, O. Christiansen, F. Engel, R. Faber, M. Heckert, O. Heun, M. Hilgenberg, C. Huber, T.-C. Jagau, D. Jonsson, J. Jusélius, T. Kirsch, K. Klein, W.J. Lauderdale, F. Lipparini, T. Metzroth, L.A. Mück, D.P. O'Neill, D.R. Price, E. Prochnow, C. Puzzarini, K. Ruud, F. Schiffmann, W. Schwalbach, C. Simmons, S. Stopkowicz, A. Tajti, J. Vázquez, F. Wang, J.D. Watts and the integral packages MOLECULE (J. Almlöf and P.R. Taylor), PROPS (P.R. Taylor), ABACUS (T. Helgaker, H.J. Aa. Jensen, P. Jørgensen, and J. Olsen), and ECP routines by A. V. Mitin and C. van Wüllen. For the current version, see http://www.cfour.de.
[25] E. Papajak, H.R. Leverentz, J. Zheng and D.G. Truhlar, J. Chem. Theory Comput. **5**, 1197–1202 (2009).
[26] T. Fornaro, M. Biczysko, J. Bloino and V. Barone, Phys. Chem. Chem. Phys. **18**, 8479–8490 (2016).
[27] M. Heckert, M. Kállay and J. Gauss, Mol. Phys. **103**, 2109–2115 (2005).
[28] S. Alessandrini, J. Gauss and C. Puzzarini, J. Chem. Theory Comput. **14**, 5360–5371 (2018).
[29] D. Feller, J. Phys. Chem. **98**, 7059–7071 (1993).
[30] T. Helgaker, W. Klopper, H. Koch and J. Noga, J. Phys. Chem. **106**, 9639 (1997).
[31] T.H. Dunning Jr., J. Chem. Phys. **90**, 1007–1023 (1989).
[32] D.E. Woon and T.H. Dunning Jr, J. Chem. Phys. **98**, 1358–1371 (1993).
[33] T.H. Dunning, K.A. Peterson and A.K. Wilson, J. Chem. Phys. **114**, 9244–9253 (2001).
[34] K.A. Peterson and T.H. Dunning Jr., J. Chem. Phys. **117**, 10548–10560 (2002).

[35] C. Puzzarini, J.F. Stanton and J. Gauss, Int. Rev. Phys. Chem. **29**, 273–367 (2010).
[36] I.M. Mills, *Vibration-Rotation Structure in Asymmetric-and Symmetric-Top Molecules* in *Molecular Spectroscopy: Modern Research* **1**, 115 (1972).
[37] H.W. Kroto, *Molecular rotation spectra*, Dover (1992).
[38] V. Barone, J. Chem. Phys. **122**, 014108 (2005).
[39] M. Piccardo, J. Bloino and V. Barone, Int. J. Quantum Chem. **115**, 948–982 (2015).
[40] M. Biczysko, P. Panek, G. Scalmani, J. Bloino and V. Barone, J. Chem. Theory Comput. **6**, 2115–2125 (2010).
[41] E. Penocchio, M. Piccardo and V. Barone, J. Chem. Theory Comput. **11**, 4689–4707 (2015).
[42] C. Puzzarini and V. Barone, Acc. Chem. Res. **51**, 548–556 (2018).
[43] R. Boussessi, N. Tasinato, A.P. Charmet, P. Stoppa and V. Barone, Mol. Phys. pp. 1–15 (2020).
[44] W. Gordy and R.L. Cook, *Microwave Molecular Spectra*, 3rd. ed. New York, Wiley (1984).
[45] M.R. Aliev and J.K.G. Watson, *Higher orther effects in the vibration-rotation spectra of semirigid molecules*, Academic Press **3**, 1–67 (1985).
[46] H.M. Pickett, J. Mol. Spectrosc. **148**, 371 – 377 (1991).
[47] D. Licari, N. Tasinato, L. Spada, C. Puzzarini and V. Barone, J. Chem. Theory Comput. **13**, 4382–4396 (2017).
[48] M.S. Schuurman, W.D. Allen, P. von Ragué Schleyer and H.F. Schaefer III, J. Chem. Phys. **122**, 104302 (2005).
[49] M. Melosso, A. Melli, L. Spada, Y. Zheng, J. Chen, M. Li, T. Lu, G. Feng, Q. Gou, L. Dore, V. Barone and C. Puzzarini, J. Phys. Chem. A **124**, 1372–1381 (2020).
[50] E. Penocchio, M. Mendolicchio, N. Tasinato and V. Barone, Can. J. Chem. **94**, 1065–1076 (2016).
[51] S. Alessandrini and C. Puzzarini, J. Phys. Chem. A **120**, 5257–5263 (2016).